EurJIC European Journal of Inorganic Chemistry
ChemPubSoc Europe
FULL PAPER

DOI:10.1002/ejic.201402970

Formation of Different Isomers of Phosphine–Imidazolyl and –Pyridyl Ruthenium(II) Complexes Affecting the Catalyst Activity in the Acceptorless Dehydrogenation of Alcohols

Robert Langer,*[a,b] Alexander Gese,[a] Donatas Gesevičius,[a] Maximilian Jost,[a] Bastian R. Langer,[a] Felix Schneck,[a] Alexander Venker,[a] and Weiqin Xu[b]

Keywords: Homogeneous catalysis / Dehydrogenation / Ruthenium / N,P ligands / Alcohols

The synthesis, reactivity, and catalytic activity of Ru^{II} complexes with different pyridine- and imidazole-based P,N ligands are reported. The investigations reveal a strong influence of the N-heterocycle and the steric demand of the phosphine groups on the stability of different isomers of $[L_2RuX_2]$ (L = P,N ligand; X = Cl, H). The imidazole-based complex **5** with dicyclohexylphosphine groups was found to be the most active precatalyst for the acceptorless dehydrogenation of primary alcohols, whereas different phosphine groups at the imidazole ligand as well as pyridine-based ligands caused a drop in catalytic activity. In the presence of a primary amine, imines are preferentially formed under these conditions. In summary, the investigations show that comparably small changes in the ligand moiety have a strong effect on the relative stability of stereoisomers for both hydride and chloride complexes, whereas isomerization of the kinetic reaction products was observed in some cases. The described changes in the ligand moiety most probably have a strong impact on the relative stabilities of isomeric intermediates as well and thus affect the catalytic activity of these complexes.

Introduction

An important concept in homogeneous catalysis takes advantage of so-called cooperative ligands or metal–ligand cooperation.[1] Thereby, the interplay of a coordinated ligand with the central metal atom of the complex allows for the reversible transfer of electrons or protons, thus leading to the application of base metal complexes as catalysts and the development of new catalytic reactions.[2]

In this context, a series of pyridine-based pincer complexes have been reported as highly efficient catalysts for various known and unknown reactions,[3] including the acceptorless dehydrogenation of primary alcohols in the presence of amines to amides and the hydrogenation of organic carbonates to methanol.[4] In particular, the reversible cleavage of dihydrogen by an aromatization–dearomatization sequence is thought to be responsible for the spontaneous liberation of H_2 in ruthenium pincer complexes (Scheme 1),[2e] whereas the typical meridional coordination mode of the pincer ligand enforces a *trans* orientation of the two hydride ligands in **I**, which seems to be favored over the carbonyl ligand *trans* to the hydride.

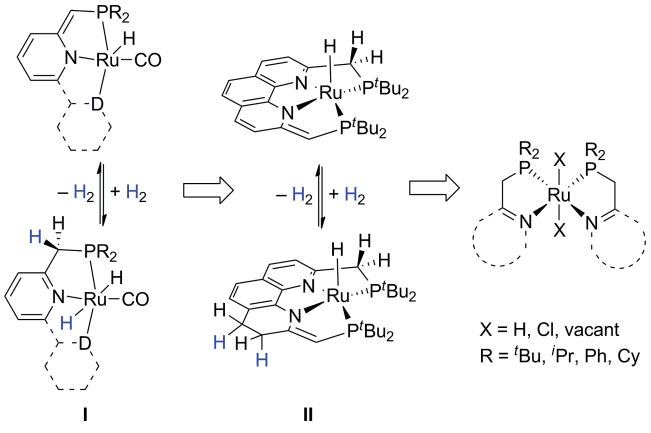

Scheme 1. Metal–ligand cooperation in H_2 activation for different ruthenium complexes and their structural relationship to P,N-ligand systems.

In addition to the generation of a reactive *trans*-dihydride intermediate, the nature of the donor group D in **I** seems to play a crucial role in the significant improvement of the catalyst activity in acceptorless dehydrogenation reactions

[a] Department of Chemistry, Philipps-Universität Marburg, Hans-Meerwein-Strasse, 35043 Marburg, Germany
E-mail: robert.langer@chemie.uni-marburg.de
http://www.uni-marburg.de/fb15/ag-langer
[b] Lehn Institute of Functional Materials (LIFM), Sun Yat-Sen University (SYSU),
Xingang Road West, Guangzhou 510275, P. R. China
Supporting information for this article is available on the WWW under http://dx.doi.org/10.1002/ejic.201402970.

of primary alcohols. Originally it was thought that this group reversibly generates a vacant coordination site, which in many cases is required for the β-hydride elimination of a coordinated alkoxide.[5] But recent experimental studies and calculations show that an outer-sphere mechanism is more likely.[6] Accordingly, Ru^{II} PNN-type pincer complexes exhibit higher activities in hydrogenation and dehydrogenation reactions than their PNP-type analogues.[3,4] In line with these findings, a similar activity is observed for Ru^{II} complexes with a tetradentate phenanthroline-based ligand **II**, which retains the *trans* orientation of the two ancillary ligands. In contrast to the pyridine-based pincer system, the intermediately formed *trans*-dihydride complex **II** undergoes reversible hydrogenation of a C=C double bond of the ligand backbone instead of H_2 liberation.[7]

As the *trans* arrangement of the phosphine groups does not seem to be crucial for the performance of the complexes, the formal deduction to two P,N ligands should also lead to active dehydrogenation catalysts with the formal composition $[L_2RuX_2]$ (X = H, Cl, vacant; L = P,N ligand). In addition, these bidentate P,N ligands are an important class of ligands that has been widely used in homogeneous catalysis.[8] Furthermore, octahedral complexes that contain two of these P,N ligands can potentially exist as different stereo- and constitutional isomers, which, for example, has been shown to be relevant for hydride complexes that can serve as active hydrogenation catalysts.[9]

For this reason, we started to investigate the coordination behavior of pyridyl- and imidazolyl-functionalized phosphine ligands towards common ruthenium precursors. Although hydrogenation reactions that employ in situ generated ruthenium catalysts with picolyl- and methylimidazolyl (^{Me}Im) phosphines have been reported, the reverse reaction has not been investigated so far.[10] However, the reaction of $[\{Ru(benzene)Cl_2\}_2]$ with one equivalent of $^{Me}ImCH_2PR_2$ (R = ^{t}Bu, Ph, *p*-Tol, Cy) initially results in the formation of $[Ru(benzene)(\eta^1\text{-}^{Me}ImCH_2PR_2)Cl_2]$, which isomerizes to the cationic complex $[Ru(benzene)(\eta^2\text{-}^{Me}ImCH_2PR_2)Cl]Cl$, thus providing evidence for the hemilabile nature of the imidazole ring.[10b] Furthermore, depending on the steric demand, phosphine-group mono- and bis-ligated complexes were obtained by the reaction of $[Ru(cod)(methylallyl)_2]$ (cod = cyclooctadiene) with two equivalents of imidazolyl phosphine and HBr.[10c] Herein, we present the synthesis and characterization of Ru^{II} complexes with the general composition $[L_2RuCl_2]$ (Scheme 2), with L denoting a pyridyl- or imidazolyl-based P,N ligand. Furthermore, we compare all complexes in the acceptorless dehydrogenation of primary alcohols and demonstrate for the most active catalyst that the imine is formed preferably in the presence of a primary amine. Finally, we investigated the impact of the heterocycle and the phosphine group by comparing the reactivity and structure of the in situ generated dihydride complexes.

Results and Discussion

Treatment of $[(Ph_3P)_3RuCl_2]$ with diisopropylphosphino(2-picolyl)phosphine (PicP^iPr_2; 2 equiv.) in dichloromethane or THF results in the formation of three different complexes according to the $^{31}P\{^1H\}$ NMR spectrum of the reaction mixture, which shows two sharp singlet resonances of different intensity at δ = 73.4 and 75.3 ppm, as well as two doublet resonances centered at δ = 68.9 and 70.4 ppm ($^2J_{P,P}$ = 29.7 Hz). Similar results were obtained when $[(cod)RuCl_2]_n$ was employed instead, thereby suggesting that no PPh_3 is present in the three newly formed complexes. On the basis of ^{1}H-COSY, ^{1}H-*g*NOESY, ^{1}H,^{13}C-HSQC, and ^{1}H,^{13}C-HMBC NMR spectroscopic experiments as well as

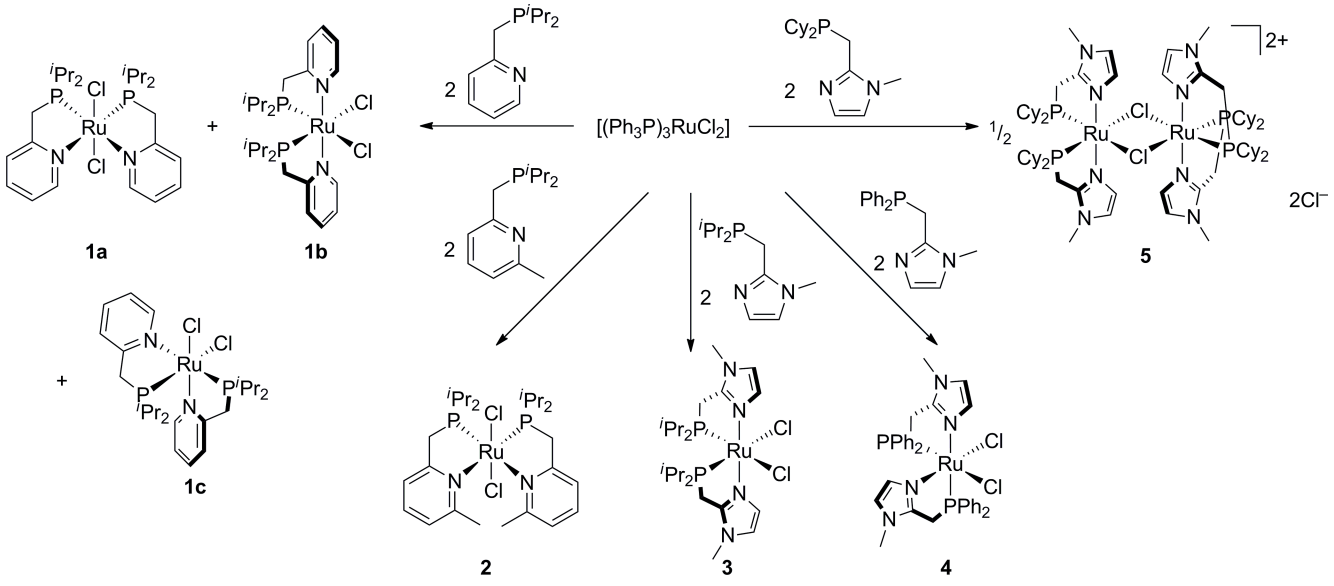

Scheme 2. Synthesis of complexes **1**–**5**.

selective ^{31}P-decoupling NMR spectroscopic experiments, assignments for the three complexes could be made, which suggested the molecular structure for **1a**–**c** shown in Scheme 2. Interestingly, no chemical exchange could be detected between the three species in the mixture by ^{1}H-*g*NOESY NMR spectroscopy, but the ratio of **1a**, **1b**, and **1c** slowly changes over the course of 20 h in CD_2Cl_2 according to the $^{31}P\{^{1}H\}$ NMR spectra.[11] All attempts to separate these complexes by crystallization failed and resulted in the formation of different types of crystals and the precipitation of a yellow powder. Nevertheless, it was possible to determine the molecular structure for two of the three complexes by means of single-crystal X-ray diffraction, thereby confirming that different $[(PicP^{i}Pr_2)_2RuCl_2]$ isomers are formed in this reaction (Figure 1a and b). The bond lengths and angles of the structurally characterized complexes are summarized in Table 1.

In the symmetric *trans*-dichloride complex **1a** the Cl1–Ru1–Cl2 angle was found to be 172.94°, whereas the two coordinated $PicP^{i}Pr_2$ ligands in the octahedral Ru^{II} complex exhibit an almost coplanar orientation with the two $P^{i}Pr_2$ groups *cis* to each other. Comparably long Ru–P distances between 2.310 and 2.312 Å are observed in complex **1a**, whereas Ru–N bond lengths range between 2.154 and 2.160 Å. The second complex was identified as the corresponding *cis*-dichlorido complex **1b** with the two pyridine rings located *trans* to each other (Figure 1b). In comparison to **1a**, the Ru–N and Ru–P distances are slightly shorter, whereas the bond length of the ruthenium–chlorine bond appears longer in **1b**.

With the aim of varying the steric and electronic properties of the P,N-ligand system, we employed the analogous 2,6-lutidine-based ligand $^{2,6}LutP^{i}Pr_2$ in the complexation of $[(Ph_3P)_3RuCl_2]$. For the corresponding $^{2,6}LutPPh_2$ ligand, Lavigne and Lugan et al. reported the formation of the *trans*-dichlorido complex, whereas with $^{2,6}LutPCy_2$ only one equivalent of ligand reacted with the Ru^{II} precursor.[12] For the ^{i}Pr-substituted ligand it turned out that, despite the increased steric repulsion of the methyl groups in the 6-position, the *trans*-dichlorido complex **2** was formed. In analogy to **1a**, the central Ru^{II} atom in **2** exhibits a distorted-octahedral environment with two coplanar $^{2,6}LutP^{i}Pr_2$ ligands ($\angle$ = 9.44°) and two chlorido ligands in the apical positions. In comparison to **1a**, the Ru–P bond lengths in **2** are slightly shorter (Table 1), whereas the Ru–N distances are elongated in **2**, possibly owing to the sterically more demanding methyl substituents. With a value of 53.62°, the tilt angle between the two pyridine groups in **2** is slightly larger than in complex **1** (45.50°).

The $^{31}P\{^{1}H\}$ NMR spectrum of **2** in C_6D_6 exhibits a single sharp peak at δ = 71.7 ppm. Contrary to these observations, very broad resonances are observed for the ^{i}Pr groups and the benzylic CH_2 groups, whereas the resonances that correspond to the pyridine ring and the CH_3 group in the 6-position of the pyridine ring appear rather sharp in the ^{1}H NMR spectrum. The ^{1}H-*g*NOESY NMR spectrum of **2** in C_6D_6 displays chemical exchange between the resonances of the ^{i}Pr groups, respectively, as well as between the two broad resonances that correspond to the benzylic CH_2 protons at δ = 3.20 and 5.12 ppm in the ^{1}H

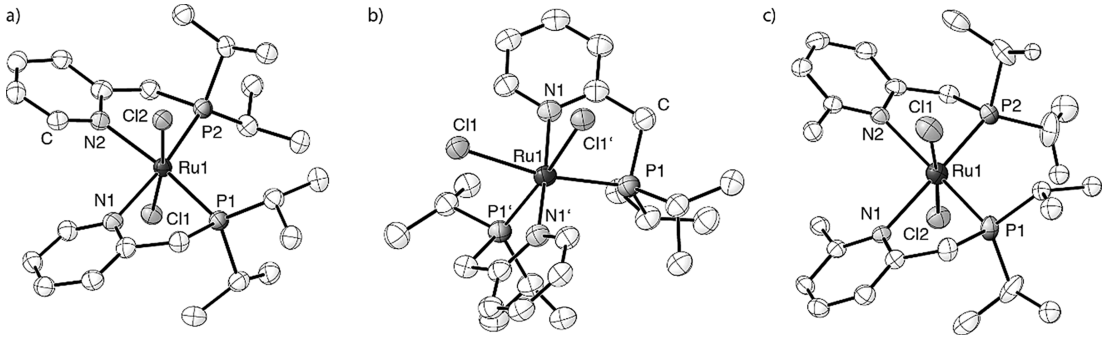

Figure 1. Molecular structures of **1a**, **1b**, and **2** obtained by single-crystal diffraction. (a) ORTEP diagram of **1a**; (b) ORTEP diagram of **1b**; and (c) ORTEP diagram of **2**. All thermal ellipsoids are set at 50% probability (hydrogen atoms were omitted for clarity).

Table 1. Selected bond lengths [Å] and angles [°] of compounds **1**–**5** for comparison.

	1a	**1b**	**2**	**3**	**4**	**5**
Ru–P	2.310–2.312	2.285	2.270–2.274	2.262–2.269	2.249–2.273	2.281–2.294
Ru–Cl	2.432–2.442	2.509	2.423–2.449	2.484–2.500	2.459–2.482	2.482–2.530
Ru–N	2.154–2.160	2.077	2.278–2.286	2.049–2.108	2.074–2.132	2.078–2.096
Cl–Ru–Cl	172.94	87.94	176.04	87.16–87.35	90.92	80.93–81.75
N–Ru–N	90.72	173.67	98.80	172.8–175.2	90.47	174.5–174.6
P–Ru–P	111.63	104.77	104.64	104.74–105.38	104.14	103.53–105.29
P_{Lig}–Ru–N_{Lig}	78.77–79.92	82.68	78.57–78.59	80.88–81.52	80.50–81.00	80.1–81.1
Het1–Ru–Het2	45.50	43.38	53.62	45.47–45.77	61.44	38.82–39.38

NMR spectrum. Such observations are in accordance with the fluxionality phosphine arms, which are able to adopt different orientations.

To further investigate the impact of the aromatic substituent on the structure, the reactivity, and the catalytic activity, we synthesized imidazolyl-based P,N ligands with a more electron-rich N-heterocycle bound to the phosphino groups. In addition to late-transition-metal complexes with imidazolyl phosphines,[13] Beller and co-workers characterized a series of complexes with the general composition [Ru(benzene)(η^2-MeImCH$_2$PR$_2$)Cl]Cl.[10b]

The analogous ^{i}Pr-substituted ligand ^{Me}ImCH$_2$P^{i}Pr$_2$ readily reacts with [(Ph$_3$P)$_3$RuCl$_2$] (0.5 equiv.) to the *cis*-dichlorido complex **3**, in which the phosphine groups are located *trans* to the two chlorido ligands (Figure 2a). The octahedral complex **3** crystallizes as a mixture of the Λ and Δ isomer in the asymmetric unit of the triclinic unit cell. The Ru–P distances in **3** are slightly longer than in **1a**, **1b**, and **2**, whereas the bonds to the nitrogen atoms of the imidazole ring are found to be shorter than in the pyridine analogues. Importantly, the same isomer as with PicP^{i}Pr$_2$ seems to be the thermodynamic product of the complexation reaction and no other isomers are formed, whereas the methyl substituent in the 6-position of ^{2,6}LutP^{i}Pr$_2$ apparently favors the *trans*-dichlorido complex. Although the resonances of the ^{i}Pr groups appear slightly broadened in the ^{1}H NMR spectrum of **3**, no chemical exchange could be detected in the ^{1}H-*g*NOESY NMR spectrum. In accordance with the determined structure, the ^{31}P{^{1}H} NMR spectrum of **3** exhibits a singlet resonance at δ = 81.1 ppm.

As small changes in the ligand moiety lead to a changed coordination behavior and different reaction products, we started to investigate the influence of the steric and electronic properties of the phosphine arm. Accordingly, the sterically less demanding and more π-accepting phosphine ^{Me}ImCH$_2$PPh$_2$ was utilized in the reaction with [(Ph$_3$P)$_3$RuCl$_2$], leading to the chiral *cis*-dichlorido complex **4**. The molecular structure of **4** has been confirmed by single-crystal X-ray diffraction (Figure 2b); it shows a chiral octahedral complex with two chlorido ligands *cis* to each other, but with different groups in the *trans* position. The corresponding bromido complex, which was published during the preparation of this manuscript, exhibits the same stereochemical configuration as complex **4**.[10c] With values of 2.249–2.273 Å, the Ru–P bond lengths were found to be almost identical with the recently reported dibromido complex. In addition, the similarity between the bromido and the chlorido complex is reflected in identical Ru–N bond lengths, whereas the ruthenium–halogen bond exhibits typical lengths for each element, respectively.

In comparison to ^{Me}ImCH$_2$P^{i}Pr$_2$, the corresponding dicyclohexylphosphine-substituted ligand ^{Me}ImCH$_2$PCy$_2$ exhibits similar electron-donating properties, whereas the bulky cyclohexyl groups cause increased steric demand. Utilizing ^{Me}ImCH$_2$PCy$_2$ in the complexation of [(Ph$_3$P)$_3$RuCl$_2$] in THF at 60 °C resulted in the formation of a yellow precipitate in 55% yield, which was identified as the dicationic dimer [(^{Me}ImCH$_2$PCy$_2$)$_4$Ru$_2$Cl$_2$]Cl$_2$ (**5**). Interestingly, when two equivalents of ^{Me}ImCH$_2$PCy$_2$ were utilized in the reaction with [Ru(cod)(methylallyl)$_2$] and HBr, only one equivalent of ligand binds to the central ruthenium atom.[10b]

The structural analysis of **5** revealed a dimeric complex with two octahedrally coordinated Ru^{II} atom, which are bridged by two μ$_2$-coordinating chlorido ligands (Figure 2c). Similar to **1b**, the phosphine groups are located *trans* to the chlorido ligands, thereby causing shortening of the Ru–P bond (2.281–2.294 Å) relative to **1a** and **2**. With values between 2.482–2.530 Å, the Ru–Cl bond lengths to the bridging chlorido ligands are very similar to the distances found in the other complexes. The imidazole rings in **5** occupy the axial positions in this dimer and are arranged in a pairwise and almost parallel manner with short distances of 3.355–3.626 Å, thus indicating π interactions between the imidazole rings.

Owing to the similarity of the ligand scaffold to other pyridine- and phenanthroline-containing ruthenium complexes, we investigated complexes **1**–**5** as precatalysts for the dehydrogenation of primary alcohols. Accordingly, in a typical experiment, a ruthenium dichlorido complex (0.01 mmol), KO^{t}Bu (0.04 mmol), and primary alcohol (5.00 mmol) in toluene (4 mL) were heated to reflux (Table 2). As the reaction proceeds rather slowly, relatively long reaction times were necessary to obtain high produc-

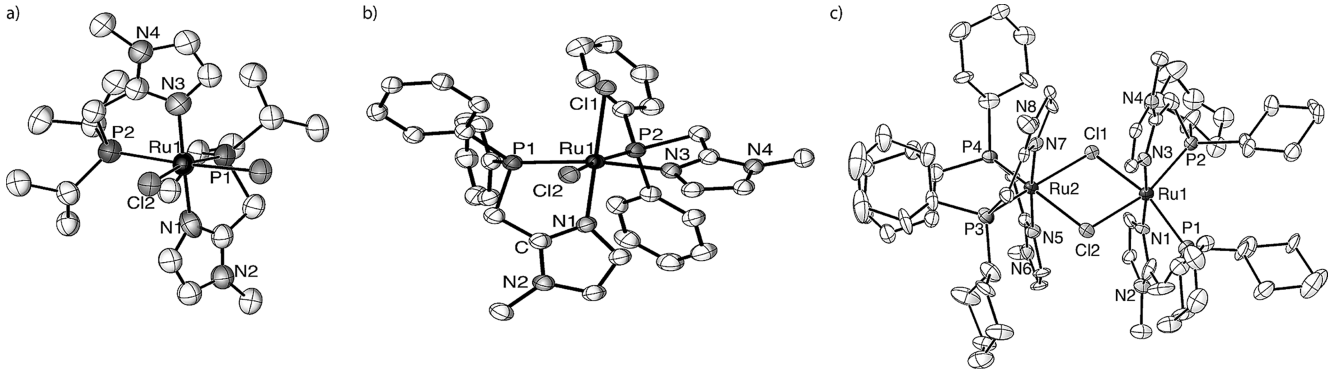

Figure 2. Molecular structures of **3**–**5** obtained by single-crystal diffraction. (a) ORTEP diagram of **3**; (b) ORTEP diagram of **4**; and (c) ORTEP diagram of **5**. All thermal ellipsoids are set at 50% probability (hydrogen atoms were omitted for clarity).

Table 2. Acceptorless dehydrogenation of primary alcohols.[a]

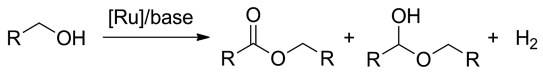

Entry	Catalyst	Alcohol	S/B/C[b]	*t* [h]	Conversion[c] [%]	Yield ester[c] [%]	Yield hemi-acetal[c] [%]
1	**1**	benzyl alcohol	500:4:1	120	63.5	38.8	24.3
2	**2**	benzyl alcohol	500:4:1	120	41.8	3.3	29.3
3	**3**	benzyl alcohol	500:4:1	120	70.3	61.7	4.4
4	**4**	benzyl alcohol	500:4:1	120	76.1	56.2	11.4
5[d]	**5**	benzyl alcohol	1000:4:1	120	95.0	63.2	31.5
6	$[(Ph_3P)_3RuCl_2]$	benzyl alcohol	500:4:1	120	36.8	2.4	32.8
7	**1**	*n*-hexanol	500:4:1	120	41.5	37.6	2.4
8	**3**	*n*-hexanol	500:4:1	120	71.1	45.0	25.4
9	**4**	*n*-hexanol	500:4:1	120	41.6	30.9	4.5
10[d]	**5**	*n*-hexanol	1000:4:1	120	93.7	68.2	19.2
11	$[(Ph_3P)_3RuCl_2]$	*n*-hexanol	500:4:1	120	43.7	0.4	6.7
12[e]	**4**	benzyl alcohol	200:4:1	19	27.4	16.8	1.2
13[e]	**5**	benzyl alcohol	400:4:1	19	93.2	35.4	46.5

[a] Reaction conditions: Alcohol (5.00 mmol), KO^{t}Bu (0.04 mmol), catalyst (0.01 mmol) and *m*-xylene (internal standard; 1.00 mmol), and toluene (4 mL) were heated to reflux for 120 h. [b] Ratio of substrate/base/catalyst. [c] Determined by GC analysis with *m*-xylene as internal standard. [d] Catalyst (0.05 mmol) was used. [e] Precatalyst (**4**: 0.01 mmol, **5**: 0.005 mmol) and KO^{t}Bu (0.04 mmol) were added under air; substrates were added under argon without purification and heated to reflux for 19 h.

tivity of the catalyst and to address selectivity issues. Employing complexes **1a**–**c** as catalyst in the dehydrogenation of benzyl alcohol gave the corresponding ester in 38.8% and the hemi-acetal in 24.3% yield (Table 2, entry 1), as detected by GC analysis. Interestingly, after removal of the solvent and the internal standard, only benzaldehyde, benzyl benzoate, and benzyl alcohol could be detected as reaction products. The hemi-acetal seems stable under the conditions of the GC and its formation is likely base-catalyzed. In a control experiment, a mixture of benzaldehyde and benzyl alcohol in toluene was heated to reflux in the presence of KO^{t}Bu; it showed a slow formation of the hemi-acetal. It is worth mentioning that homogeneous catalysts capable of dehydrogenating a primary alcohol to an aldehyde are rare.[14]

Interestingly, the methyl-substituted complex **2** exhibits a significantly lower catalytic productivity in the dehydrogenation reaction, in which only 3.3% of benzyl benzoate and 29.3% of benzaldehyde hemi-acetal are formed (Table 2, entry 2). With a conversion of 70.3%, the imidazolyl-based complex *cis*-$[(^{Me}ImCH_2P^iPr_2)_2RuCl_2]$ (**3**) exhibits a productivity similar to its pyridine-based counterpart (**1a**–**c**), but the selectivity for the ester formation is increased. A similar observation can be made for the phenyl-substituted analogue **4**, which results in a conversion of 76.1% when employed as a catalyst in the dehydrogenation of benzyl alcohol (Table 2, entry 4). In comparison to **3**, with **4** as catalyst slightly less of the ester and more of the hemi-acetal is formed. The highest catalytic activity was observed with complex **5** as catalyst, which resulted in 95% conversion of the benzyl alcohol (Table 2, entry 5). When the reaction was stopped after 66 h, 69.0% conversion of benzyl alcohol was detected by means of GC analysis. Thus, complex **5** exhibits a similar catalytic activity to the previously reported complex **II** with a four-dentate and phenanthroline-based ligand.[8] Importantly, at 63.2%, the yield of benzyl benzoate is similar to **3** and **4** but the hemi-acetal is formed in much higher yield. For comparison we utilized the non-functionalized precursor complex $[(Ph_3P)_3RuCl_2]$ as catalyst for the dehydrogenation of benzyl alcohol (Table 2, entry 6). To our surprise, the reaction resulted in 36.8% conversion of benzyl alcohol, but the hemi-acetal is formed almost exclusively. Thus, complex **2** and $[(Ph_3P)_3RuCl_2]$ exhibit similar catalytic activities and selectivities in the acceptorless dehydrogenation of benzyl alcohol. In accordance with the discussed hemi-acetal formation, the catalytic dehydrogenation of a mixture of benzaldehyde and benzyl alcohol with complex **5** as catalyst results in the conversion of both substrates and subsequent ester formation. Moreover, the continuous GC analysis of the reaction with complex **5** as catalyst revealed that after a short period the concentration of aldehyde and hemi-acetal remained constant over the course of the reaction.

The reaction with *n*-hexanol as substrate resulted in much lower conversion of 41.5% with **1** as catalyst but gave a similar yield of the corresponding ester (Table 2, entry 7). When the imidazole-based complex **3** was employed in the reaction, 71.1% conversion of *n*-hexanol was observed, but only 45.0% of hexyl hexanoate was formed during this reaction (Table 2, entry 8). The phenyl-substituted complex **4** appears less active for the dehydrogenation of *n*-hexanol and gave only 41.6% conversion (Table 2, entry 9). In line with the observations for **3**, 93.7% conversion of *n*-hexanol was detected with complex **5** as a catalyst (Table 2, entry 10), whereas the ester was formed in 68.3% and the corresponding hemi-acetal in 19.2% yield. Finally, we investigated the activity of the precursor complex $[(Ph_3P)_3RuCl_2]$ as catalyst, which resulted in 43.7% conversion of *n*-hexanol, but the major product of the reaction turned out to be 2-butyl octanol (Table 2, entry 11), which is likely formed by aldol condensation of hexanal followed by hydrogenation of the formed α,β-unsaturated aldehyde.

As the imidazole-based dichlorido ruthenium complexes did not show any sign of decomposition in the presence of oxygen and moisture after two weeks, we investigated the possibility of using these complexes as bench-stable precatalysts under air. In a typical experiment, complex **4** or **5**, which had been stored under air for several days, was weighted into a Schlenk tube together with the required amount of KO^{t}Bu. The tube was evacuated and refilled with argon and benzyl alcohol, then *m*-xylene and toluene were added to the Schlenk tube under a stream of argon without any kind of purification or degassing of these compounds. With 27.4% conversion of the primary alcohol, complex **4** showed poor performance after heating the mixture to reflux for 19 h (Table 2, entry 12). To our surprise, with 0.25 mol-% of **5** as precatalyst, 93.2% conversion of benzyl alcohol was observed after 19 h (Table 2, entry 13). Interestingly, the corresponding hemi-acetal was the main product of this reaction, whereas benzyl benzoate was formed in only 35.4% yield.

In the presence of primary amines, different products have been reported for different catalysts in the acceptorless dehydrogenation (Scheme 3).[15] These range from N-heterocyclic compounds[16] to secondary amines,[17] imines,[18] and amides.[4a,19,20] For this reason we investigated the most active complex of this series, complex **5**, as a dehydrogenation catalyst in the presence of a primary amine (Scheme 4). Notably, the conversion of benzyl alcohol decreased in the presence of benzylamine but resulted in selective formation of the imine (39.0%). In contrast to the imine formation, which is assumed to take place in a noncatalytic dehydration step of the generated aldehyde and the primary amine, the generation of amides or esters requires an additional dehydrogenation step of the in situ formed hemi-aminal or the hemi-acetal, respectively.[3c,21] Accordingly, with higher catalyst loading (0.2 mol-%), complete conversion of benzyl alcohol was observed, but a very unselective product distribution with almost equal amounts of imine, ester, and amide was obtained. Notably, almost no secondary amine (<0.5%) was observed in these reactions.

In addition to determining the catalytic activity of the dichlorido complexes, we aimed to compare the reactivity and stability of the corresponding dihydride complexes with the analogous complexes that contained three- and fourdentate ligands. Several mechanistic investigations of different ruthenium catalysts for the acceptorless dehydrogenation of primary alcohols and related reactions have been conducted, thus indicating that *trans*-dihydridoruthenium(II) complexes are usually intermediates in the catalytic

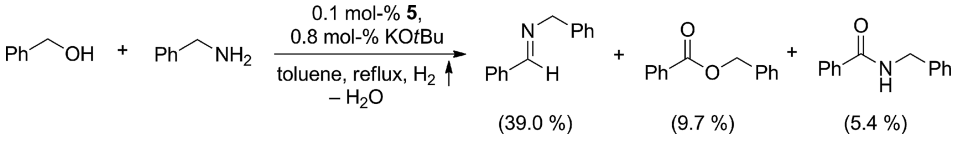

Scheme 3. Acceptorless dehydrogenation of benzyl alcohol in the presence of benzylamine.

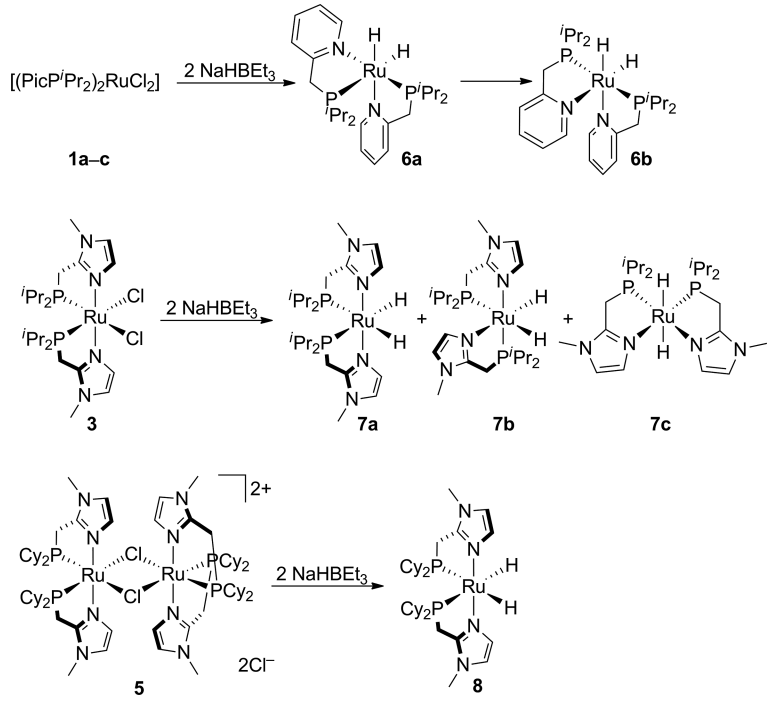

Scheme 4. Formation of hydride complexes.

cycle.[22] For this reason, we treated the synthesized dichlorido complexes with two equivalents of a hydride transfer reagent, such as $NaHBEt_3$ in C_6D_6. It turned out that the generated hydride complexes under discussion were not isolable as pure compounds. In spite of this, a possible structure of the formed complexes was suggested on the basis of ^1H, $^1H\{^{31}P\}$, and ^1H-*g*COSY NMR spectroscopy.

When **1a**–**c** were treated with two equivalents of $NaHBEt_3$ (0.5 M in C_6D_6), the solution immediately decolorized and the $^{31}P\{^1H\}$ NMR spectrum indicated the formation of a new ruthenium complex, which was identified as the *cis*-dihydride complex **6a**. In solution, complex **6a** is slowly converted to another hydride complex, the NMR spectra of which are in agreement with the formation of complex **6b**. Selected NMR spectroscopic chemical shifts for the prepared hydride complexes are summarized in Table 3.

Table 3. Selected NMR chemical shifts for the hydride complexes **6**–**8**.

	$^{31}P\{^1H\}$ NMR [ppm]	^1H NMR [ppm]	$^2J_{P,H}$ [Hz][a]	$^2J_{H,H}$ [Hz][a]
6a	67.9 (d), 96.5 (d)	–16.83 (vtd)	21.9	8.5
	($^2J_{P,P}$ = 14.8 Hz)	–7.52 (ddd)	91.4, 25.6	8.5
6b	88.4 (s)	–14.77 (t)	20.1	–
7a	72.7 (s)	–7.68 (m)	–	–
7b	76.4 (d), 103.9 (d)	–17.95 (vtd)	32.9	8.5
	($^2J_{P,P}$ = 14.8 Hz)	–7.76 (ddd)	97.5, 24.4	8.5
7c	82.5 (s)	–9.14 (t)	17.1	–
8	64.2 (s)	–7.79 (m)		–

[a] Coupling constant of the resonance corresponding to the hydride ligand.

The isomerization of ruthenium hydride complexes was shown to be relevant for ruthenium diamine diphosphine complexes, in which the corresponding *trans*-dihydride complex was found to be the active species, and which exhibits a limited lifetime and isomerizes to the corresponding *cis*-dihydride complexes.[9] This is of particular importance because for some ruthenium catalysts the *cis* and the *trans* isomer of hydride complexes are calculated to have similar energy but exhibit significantly different reaction barriers within the catalytic cycle.[22b]

Whereas with the pyridine-based P,N ligand the chiral complex **6a** is initially formed as the kinetic product, which slowly converts into the symmetric hydride complex **6b**, the situation changed for the imidazole-based ligands. Treatment of complex **3** with $NaHBEt_3$ (2 equiv.) in C_6D_6 resulted in the formation of a mixture of three isomeric dihydride complexes (**7a**–**c**), whereas the ratio of these complexes did not change for several weeks. In contrast, the same reaction with complex **5** led to a single product (**8**), as indicated by a singlet resonance at δ = 64.2 ppm in the $^{31}P\{^1H\}$ NMR spectrum. Complexes **7a** and **8** show very similar patterns in the ^1H NMR spectrum for the resonance that corresponds to the imidazole moiety and the hydride ligands (Figure 3c and d). On the basis of one- and two-dimensional NMR spectroscopy, the *cis*-dihydride isomer with the two phosphine groups in a *trans* position to them is assumed for both complexes. The two other products from the reaction of **3** with two equivalents of $NaHBEt_3$ were identified as the chiral *cis*-dihydride **7b** and a *trans*-dihydride complex (**7c**), with the assumed structure shown in Scheme 4.

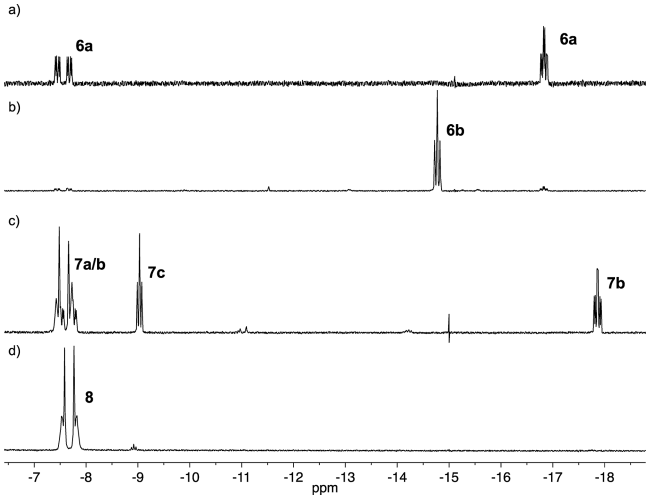

Figure 3. ^1H NMR spectra of the dihydride complexes **6**–**8** in C_6D_6: (a) **1a**–**c** + $NaHBEt_3$ (2 equiv.) after 5 min; (b) **1a**–**c** + $NaHBEt_3$ (2 equiv.) after 18 h; (c) **3** + $NaHBEt_3$ (2 equiv.); and (d) **5** + $NaHBEt_3$ (2 equiv.).

However, in all cases the in situ formed dihydride complexes **6**–**8** appeared stable in solution for several days without any sign of dihydrogen elimination, but they are converted into a mixture of unidentified products after workup, including removal of all volatiles under vacuum. Furthermore, the addition of a primary alcohol such as benzyl alcohol or methanol to these complexes resulted in immediate gas evolution of dihydrogen and the formation of a new complex, respectively. In the case of complex **8**, the newly formed complex after addition of benzyl alcohol gave rise to a broadened resonance at δ = 78.6 ppm in the $^{31}P\{^1H\}$ NMR spectrum. In the corresponding ^1H NMR spectrum, two broad resonances at δ = –10.57 and –1.17 ppm were observed. Notably, heating of this mixture to 70 °C for one hour resulted in the evolution of a new resonance at δ = 85.9 ppm in the $^{31}P\{^1H\}$ NMR spectrum and a new resonance at δ = –21.77 ppm for the corresponding hydride ligand in the ^1H NMR spectrum. Addition of CD_3OD to the dihydride complexes caused gas evolution as well and resulted in the formation of the analogous complexes, but no deuterium incorporation into the P,N ligand could be observed after several days. In contrast to the reactivity of the Ru^{II} complexes with rigid three- and four-dentate ligands, in which a *trans*-dihydride complex or a reaction product thereof can be observed, the more flexible bidentate P,N ligands allow for the formation of different *cis*-dihydride complexes, which could generally be formed by isomerization of an initially formed *trans*-dihydride complex.

For comparison we investigated the reaction mixture of a catalytic dehydrogenation experiment by NMR spectroscopy. Complex **5** was treated with KO^{t}Bu (2 equiv.) and benzyl alcohol (50 equiv.) in toluene or C_6D_6. Initially, a new complex with a chemical shift of δ = 80.4 ppm in the $^{31}P\{^1H\}$ NMR spectrum was formed. The absence of a hydride resonance in the ^1H NMR spectrum might indicate the formation of a symmetric alkoxide complex. Upon heating to at least 70 °C, a new complex was formed within minutes with a chemical shift of δ = 83.2 ppm in the $^{31}P\{^1H\}$ NMR spectrum. The newly formed complex exhibits a broad resonance at δ = –22.60 ppm with an integral of one in its ^1H NMR spectrum, which corresponded to a hydride ligand. The chemical shift of δ = –22.60 ppm is quite similar to those observed after the addition of benzyl alcohol to complex **8** and indicates the presence of a weak donor ligand, such as an alcohol or an alkoxide, *trans* to the hydride. Notably, prolonged heating of the mixture did not change this situation. That no dihydride complexes can be observed in the presence of alcohols and the fact that the separately prepared dihydride complexes readily liberate H_2 upon treatment with alcohol indicates that the observed hydride alkoxide species likely represents the catalytic resting state. The experiments with CD_3OD showed that no deuterium incorporation into the P,N ligand takes place, thus suggesting that none of the ligand protons is involved in hydrogen generation and that an intermediate dihydrogen complex is probably formed by simple protonation of the dihydride.

As the comparably small changes in the ligand moiety have a strong effect on the relative stability of stereoisomers, for both hydride and chloride complexes, it seems likely that the relative stabilities of possible intermediates (on and off cycle) are also strongly affected by these changes and thus cause different catalytic performance. Whereas complexes with rigid ligand systems are rather limited in their possible stereoisomers, the use of flexible P,N ligands has led to different isomeric species that involve isomerization equilibria.

Conclusion

In conclusion, we have described the synthesis and reactivity of Ru^{II} complexes with different P,N ligands, thereby demonstrating the influence of the N-heterocycle as well as the influence of the steric and electronic properties of the phosphine on the relative stability of different isomers of the type $[L_2RuX_2]$ (L = P,N ligand; X = Cl, H). Among the investigated complexes, the bench-stable precatalyst **5** exhibits the highest catalytic activity in the dehydrogenation of primary alcohols to esters and is able to catalyze the direct transformation of alcohols to imines in the presence of amines. The reactivity studies with the corresponding hydride complexes provide evidence for a non-cooperative mechanism in which a hydrido alkoxide species appears to be the catalytic resting state. In addition, our investigations show that small changes in the ligand moiety strongly affect the stability of different isomers as well as the catalytic activity of the synthesized precatalysts. We could demonstrate in part that kinetic reaction products slowly isomerize to thermodynamically stable isomers at ambient temperature. Overall, the relative stabilities of isomeric intermediates are likely influenced by the changes in the ligand moiety and thus cause a different catalytic performance.

Experimental Section

General: All experiments were carried out under an atmosphere of purified argon or nitrogen in a Braun Labmaster glovebox or by using standard Schlenk techniques. CH_2Cl_2 was dried with CaH_2, toluene was dried with sodium, and THF was dried with Na/K alloy. C_6D_6 was distilled from Na/K alloy and stored over molecular sieves; all other deuterated solvents were sparged with argon and stored over molecular sieves. $[(Ph_3P)_3RuCl_2]$,[23] $[(cod)RuCl_2]_n$,[24] and the P,N ligands were prepared according to previously reported procedures.[12,13d] Benzyl alcohol and *n*-hexanol were purchased from Aldrich, degassed, and stored in the glovebox under an inert atmosphere. Detailed procedures for the synthesis of all complexes including all spectroscopic data can be found in the Supporting Information.

^1H, ^{13}C, and ^{31}P NMR spectra were recorded with a Bruker DRX 400 or a DPX 250 NMR spectrometer. ^1H and $^{13}C\{^1H\}$, ^{13}C-APT (attached proton test) NMR spectroscopic chemical shifts are reported in ppm downfield from tetramethylsilane. The resonance of the residual protons in the deuterated solvent was used as internal standard for ^1H NMR spectroscopy. The solvent peak of the deuterated solvent was used as internal standard for ^{13}C NMR spectroscopy. ^{31}P NMR spectroscopic chemical shifts are reported in ppm downfield from H_3PO_4 and referenced to an external 85% solution of phosphoric acid in D_2O. IR spectra were recorded by attenuated total reflection of the solid samples with a Bruker Tensor IF37 spectrometer. HR-ESI mass spectra were acquired with a LTQ-FT mass spectrometer (Thermo Fischer Scientific), as were HR-APCI mass spectra. In both cases the resolution was set to 100000. Elemental analyses were performed with a Vario Micro Cube Elemental Analyzer. Gas chromatography was performed with *m*-xylene as internal standard with an HP-5 column and an Agilent 6850 series GC system.

Single-Crystal X-ray Analysis: The single-crystal X-ray diffraction data for the structural analysis of **1a**, **1b**·THF, **2**·0.5THF, **3**·2.5CH_2Cl_2, **4**·3CH_2Cl_2, and **5**·3$CHCl_3$ were collected using graphite-monochromated Mo-K_α radiation (λ = 0.71073 Å) with a STOE IPDS2 or IPDS2T imaging plate detector system. The structures were solved by direct methods with SHELXS-97 and refined against F^2 by full-matrix least-square techniques using SHELXL-97.[25] Numerical absorption corrections were applied on the basis of the crystal descriptions.[26]

CCDC-994528 (for **1a**), -994529 (for **1b**·THF), -994530 (for **2**·0.5THF), -994531 (for **3**·2.5CH_2Cl_2), -994532 (for **4**·3CH_2Cl_2), and -994533 (for **5**·3$CHCl_3$) contain the supplementary crystallographic data for this paper. These data can be obtained free of charge from The Cambridge Crystallographic Data Centre via www.ccdc.cam.ac.uk/data_request/cif.

Dehydrogenation of Primary Alcohols: In a typical experiment, catalyst (0.01 mmol), KO^{t}Bu (0.04 mmol), primary alcohol (5.00 mmol), *m*-xylene (1.00 mmol), and toluene (4 mL) were placed in a Schlenk tube under nitrogen atmosphere. In the case of the dimeric complex **5**, 0.005 mmol was used in the catalytic reaction. The mixture was heated to reflux for the specified time, and

the extent of conversion was frequently checked by GC analysis. After the reaction, the mixture was cooled to ambient temperature and the mixture was analyzed by GC.

Supporting Information (see footnote on the first page of this article): Details of the data collection and the refinement are described in the Supporting Information.

Acknowledgments

R. L. is grateful to Prof. S. Dehnen and Prof. C. v. Hänisch for their continuous support and assistance. This research is supported by the Erich Becker Foundation. W. X. received a PhD fellowship from the National Natural Science Foundation of China (NSFC).

[1] a) H. Grützmacher, *Angew. Chem. Int. Ed.* **2008**, *47*, 1814–1818; *Angew. Chem.* **2008**, *120*, 1838–1842; b) S. Schneider, J. Meiners, B. Askevold, *Eur. J. Inorg. Chem.* **2012**, *3*, 412–429; c) J. I. van der Vlugt, *Eur. J. Inorg. Chem.* **2012**, *3*, 363–375; d) D. Milstein, *Top. Catal.* **2010**, *53*, 915–923; e) C. Gunanathan, D. Milstein, *Science* **2013**, *341*, 249–261.

[2] a) S. Schneider, J. Meiners, B. Askevold, *Eur. J. Inorg. Chem.* **2012**, 412–429; b) D. Gelman, S. Musa, *ACS Catal.* **2012**, *2*, 2456–2466; c) S. Kuwata, T. Ikariya, *Chem. Commun.* **2014**, *50*, 14290–14300; d) V. T. Annibale, D. Song, *RSC Adv.* **2013**, *3*, 11432–11449; e) C. Gunanathan, D. Milstein, *Acc. Chem. Res.* **2011**, *44*, 588–602.

[3] a) J. Zhang, G. Leitus, Y. Ben-David, D. Milstein, *J. Am. Chem. Soc.* **2005**, *127*, 10840–10840; b) E. Balaraman, B. Gnanaprakasam, L. J. W. Shimon, D. Milstein, *J. Am. Chem. Soc.* **2010**, *132*, 16756–16758; c) B. Gnanaprakasam, J. Zhang, D. Milstein, *Angew. Chem. Int. Ed.* **2010**, *49*, 1468–1471; *Angew. Chem.* **2010**, *122*, 1510–1513; d) C. Gunanathan, L. J. W. Shimon, D. Milstein, *J. Am. Chem. Soc.* **2009**, *131*, 3146–3147; e) B. Gnanaprakasam, D. Milstein, *J. Am. Chem. Soc.* **2011**, *133*, 1682–1685; f) B. Gnanaprakasam, E. Balaraman, Y. Ben-David, D. Milstein, *Angew. Chem. Int. Ed.* **2011**, *50*, 12240–12244; *Angew. Chem.* **2011**, *123*, 12448–12452; g) C. Gunanathan, D. Milstein, *Angew. Chem. Int. Ed.* **2008**, *47*, 8661–8664; *Angew. Chem.* **2008**, *120*, 8789.

[4] a) C. Gunanathan, Y. Ben-David, D. Milstein, *Science* **2007**, *317*, 790–792; b) E. Balaraman, C. Gunanathan, J. Zhang, L. J. W. Shimon, D. Milstein, *Nat. Chem.* **2011**, *3*, 609–614.

[5] a) O. Blum, D. Milstein, *J. Organomet. Chem.* **2000**, *593–594*, 479–484; b) C. M. Fafard, O. V. Ozerov, *Inorg. Chim. Acta* **2007**, *360*, 286–292; c) N. A. Smythe, K. A. Grice, B. S. Williams, K. I. Goldberg, *Organometallics* **2009**, *28*, 277–288; d) J. C. M. Ritter, R. G. Bergman, *J. Am. Chem. Soc.* **1998**, *120*, 6826–6827.

[6] a) M. Montag, J. Zhang, D. Milstein, *J. Am. Chem. Soc.* **2012**, *134*, 10325–10328; b) S. Qu, Y. Dang, C. Song, M. Wen, K.-W. Huang, *J. Am. Chem. Soc.* **2014**, *136*, 4974–4991; c) H. Li, X. Wang, F. Huang, G. Lu, J. Jiang, Z.-X. Wang, *Organometallics* **2011**, *30*, 5233–5247; d) H. Li, X. Wang, M. Wen, Z.-X. Wang, *Eur. J. Inorg. Chem.* **2012**, 5011–5020.

[7] R. Langer, I. Fuchs, M. Vogt, E. Balaraman, Y. Diskin-Posner, G. Leitus, L. J. W. Shimon, Y. Ben-David, D. Milstein, *Chem. Eur. J.* **2013**, *19*, 3407–3414.

[8] M. P. Carrol, P. J. Guiry, *Chem. Soc. Rev.* **2014**, *43*, 819–833, and references cited therein.

[9] R. Abbel, K. Abdur-Rashid, M. Faatz, A. Hadzovic, A. J. Lough, R. H. Morris, *J. Am. Chem. Soc.* **2005**, *127*, 1870–1882.

[10] a) T. Miura, I. E. Held, S. Oishi, M. Naruto, S. Saito, *Tetrahedron Lett.* **2013**, *54*, 2674–2678; b) K. Junge, B. Wendt, F. A. Westerhaus, A. Spannenberg, H. Jiao, M. Beller, *Chem. Eur. J.* **2012**, *18*, 9011–9018; c) S. Werkmeister, K. Junge, B. Wendt, A. Spannenberg, H. Jiao, C. Bornschein, M. Beller, *Chem. Eur. J.* **2014**, *20*, 4227–4231.

[11] For details, please see the Supporting Information.

[12] E. Mothes, S. Sentets, M. A. Luquin, R. Mathieu, N. Lugan, G. Lavigne, *Organometallics* **2008**, *27*, 1193–1206.

[13] a) L. D. Field, B. A. Messerle, K. Q. Vuonga, P. Turner, *Dalton Trans.* **2009**, 3599–3614; b) H.-F. Lang, P. E. Fanwick, R. A. Walton, *Inorg. Chim. Acta* **2002**, *329*, 9–12; c) M. A. Jalil, S. Fujinami, H. Nishikawa, *J. Chem. Soc., Dalton Trans.* **2001**, 1091–1098; d) M. A. Jalil, S. Fujinami, H. Senda, H. Nishikawa, *J. Chem. Soc., Dalton Trans.* **1999**, 1655–1661.

[14] a) R. Kawahara, K. Fujita, R. Yamaguchi, *Angew. Chem. Int. Ed.* **2012**, *51*, 12790–12794; b) K. Fujita, T. Yoshida, Y. Imori, R. Yamaguchi, *Org. Lett.* **2011**, *13*, 2278–2281; c) R. Kawahara, K. Fujita, R. Yamaguchi, *J. Am. Chem. Soc.* **2012**, *134*, 3643–3646.

[15] a) G. E. Dobereiner, R. H. Crabtree, *Chem. Rev.* **2010**, *110*, 681–703; b) G. Guillena, D. J. Ramón, M. Yus, *Chem. Rev.* **2010**, *110*, 1611–1641.

[16] a) S. Michlik, R. Kempe, *Angew. Chem. Int. Ed.* **2013**, *52*, 6326–6329; b) S. Michlik, R. Kempe, *Nat. Chem.* **2013**, *5*, 140–144; c) D. Srimani, Y. Ben-David, D. Milstein, *Angew. Chem. Int. Ed.* **2013**, *52*, 4012–4015.

[17] a) F. E. Fernández, M. C. Puerta, P. Valerga, *Organometallics* **2012**, *31*, 6868–6879; b) D. Hollmann, A. Tillack, D. Michalik, R. Jackstell, M. Beller, *Chem. Asian J.* **2007**, *2*, 403–410; c) A. Del Zotto, W. Baratta, M. Sandri, G. Verardo, P. Rigo, *Eur. J. Inorg. Chem.* **2004**, 524–529; d) B. Blank, M. Madalska, R. Kempe, *Adv. Synth. Catal.* **2008**, *350*, 749–758; e) M. Haniti, S. A. Hamid, J. M. J. Williams, *Chem. Commun.* **2007**, 725–727; f) R. Grigg, T. R. B. Mitchell, S. Sutthivaiyakit, N. Tongpeny, *J. Chem. Soc., Chem. Commun.* **1981**, 611–612; g) M. H. S. A. Hamid, C. L. Allen, G. W. Lamb, A. C. Maxwell, H. C. Maytum, A. J. A. Watson, J. M. J. Williams, *J. Am. Chem. Soc.* **2009**, *131*, 1766–1774; h) Y. Watanabe, Y. Tsuji, H. Ige, Y. Ohsugi, T. Ohta, *J. Org. Chem.* **1984**, *49*, 3359–3363; i) Y. Watanabe, Y. Morisaki, T. Kondo, T. Mitsudo, *J. Org. Chem.* **1996**, *61*, 4214–4218; j) D. Gnanamgari, E. L. O. Sauer, N. D. Schley, C. Butler, C. D. Incarvito, R. H. Crabtree, *Organometallics* **2009**, *28*, 321–325.

[18] a) N. D. Schley, G. E. Dobereiner, R. H. Crabtree, *Organometallics* **2011**, *30*, 4174–4179; b) C. Chen, Y. Zhang, S. H. Hong, *J. Org. Chem.* **2011**, *76*, 10005–10010; c) A. Maggi, R. Madsen, *Organometallics* **2012**, *31*, 451–455; d) M. A. Esteruelas, N. Honczek, M. Oliván, E. Oñate, M. Valencia, *Organometallics* **2011**, *30*, 2468–2471; e) Y. Nakajima, Y. Okamoto, Y.-H. Chang, F. Ozawa, *Organometallics* **2013**, *32*, 2918–2925; f) C. Xu, L. Y. Goh, S. A. Pullarkat, *Organometallics* **2011**, *30*, 6499–6502.

[19] a) L. U. Nordstrøm, H. Vogt, R. Madsen, *J. Am. Chem. Soc.* **2008**, *130*, 17672–17673; b) J. H. Dam, G. Osztrovszky, L. U. Nordstrøm, R. Madsen, *Chem. Eur. J.* **2010**, *16*, 6820–6827; c) M. H. G. Prechtl, K. Wobser, N. Theyssen, Y. Ben-David, D. Milstein, W. Leitner, *Catal. Sci. Technol.* **2012**, *2*, 2039–2042.

[20] a) S. C. Ghosh, S. Muthaiah, Y. Zhang, X. Xu, S. H. Hong, *Adv. Synth. Catal.* **2009**, *351*, 2643–2649; b) S. C. Ghosh, S. H. Hong, *Eur. J. Org. Chem.* **2010**, 4266–4270; c) S. Muthaiah, S. C. Ghosh, J.-E. Jee, C. Chen, J. Zhang, S. H. Hong, *J. Org. Chem.* **2010**, *75*, 3002–3006; d) Y. Zhang, C. Chen, S. C. Ghosh, Y. Li, S. H. Hong, *Organometallics* **2010**, *29*, 1374–1378; e) C. Chen, S. H. Hong, *Org. Biomol. Chem.* **2011**, *9*, 20–26; f) J. Zhang, M. Senthilkumar, S. C. Ghosh, S. H. Hong, *Angew. Chem. Int. Ed.* **2010**, *49*, 6391–6393.

[21] H. Li, X. Wang, M. Wen, Z.-X. Wang, *Eur. J. Inorg. Chem.* **2012**, 5011–5020.

[22] a) X. Yang, *ACS Catal.* **2013**, *3*, 2684–2688; b) I. S. Makarov, P. Fristrup, R. Madsen, *Chem. Eur. J.* **2012**, *18*, 15683–15692; c) M. Montag, J. Zhang, D. Milstein, *J. Am. Chem. Soc.* **2012**, *134*, 10325–10328; d) D. Cho, K. Chul Ko, J. Y. Lee, *Organometallics* **2013**, *32*, 4571–4576; e) K. S. Sandhya, C. H. Suresh, *Organometallics* **2013**, *32*, 2926–2933.

[23] P. S. Hallman, T. A. Stephenson, G. Wilkinson, *Inorg. Synth.* **1970**, *12*, 237–240.
[24] M. O. Albers, E. Singleton, J. E. Yates, *Inorg. Synth.* **1989**, *26*, 249–258.
[25] G. M. Sheldrick, *Acta Crystallogr., Sect. A* **2008**, *64*, 112–122.
[26] a) X-SHAPE, v. 1.06, *Crystal Optimisation for Numerical Absorption Correction Program*, Stoe & Cie GmbH, Darmstadt, Germany, **1999**; b) X-RED32, v. 1.01, *Data Reduction Program*, Stoe & Cie GmbH, Darmstadt, Germany, **2001**.

Received: October 09, 2014
Published Online: January 19, 2015

